Radial Dependence of the Nucleon Effective Mass in ^{10}B

L. J. de Bever,[1,2] H. P. Blok,[1,3] R. S. Hicks,[4] C. W. de Jager,[1,5] N. Kalantar-Nayestanaki,[3,6] J. J. Kelly,[7] L. Lapikás,[1] R. A. Miskimen,[4] D. Van Neck,[6,8] G. A. Peterson,[4] G. van der Steenhoven,[1] and H. de Vries[1]

[1]*Nationaal Instituut voor Kernfysica en Hoge-Energiefysica (NIKHEF), P.O. Box 41882, 1009 DB Amsterdam, The Netherlands*

[2]*Departement für Physik und Astronomie der Universität Basel, Klingelbergstrasse 82, 4056 Basel, Switzerland*

[3]*Department of Physics and Astronomy, Vrije Universiteit, 1081 HV Amsterdam, The Netherlands*

[4]*Department of Physics and Astronomy, University of Massachusetts, Amherst, Massachusetts 01003*

[5]*Thomas Jefferson National Accelerator Facility, Newport News, Virginia 23606*

[6]*Kernfysisch Versnellerinstituut, Rijksuniversiteit Groningen, 9747 AA Groningen, The Netherlands*

[7]*Department of Physics, University of Maryland, College Park, Maryland 20742*

[8]*Department of Subatomic and Radiation Physics, Rijksuniversiteit Gent, 9000 Gent, Belgium*

(Received 22 August 1997)

The dynamic properties of the atomic nucleus depend strongly on correlations between the nucleons. We present a combined analysis of inelastic electron-scattering data and electron-induced proton knockout measurements in an effort to obtain phenomenological information on nucleon-nucleon correlations. Our results indicate that the ratio of radial wave functions extracted from precise $^{10}\mathrm{B}(e,e')$ and $^{10}\mathrm{B}(e,e'p)$ measurements evolve from an interior depression for small E_m, characteristic of short-range correlations, to a surface-peaked enhancement for larger E_m, characteristic of long-range correlations. This observation can be interpreted in terms of the nucleon effective mass. [S0031-9007(98)06023-2]

PACS numbers: 25.30.Fj, 14.20.Dh, 25.30.Dh, 27.20.+n

The independent-particle shell model (IPSM) of the atomic nucleus is remarkably successful in describing a variety of nuclear properties. In particular, IPSM wave functions give a good account of single-nucleon transfer and knockout measurements, such as obtained with the quasielastic $(e,e'p)$ reaction [1–3], up to the Fermi momentum ($k_F \approx 250$ MeV/c). Nonetheless, single-particle spectroscopic factors deduced from $(e,e'p)$ data are found to be systematically smaller than IPSM predictions [4–6]. This quenching has led to notions such as quasiparticle wave functions and effective masses, concepts for describing the effects of nuclear binding and correlations between nucleons that spread out the spectroscopic strength over large energy and momentum ranges [7,8].

The local effective nucleon mass $m^*(r,E)/m$ may be defined as the product of two components, the k mass and the E mass, according to $m^*(r,E)/m = [m_k(r,E)/m][m_E(r,E)/m]$. The k mass takes into account the nonlocality of the nuclear mean field by means of an additional energy (E) dependence, and resembles the well-known Perey factor. The E mass describes the coupling of hole states to low-lying collective excitations of the target nucleus (long-range correlations, LRC) as well as the effect of short-range correlations (SRC) and of tensor correlations. In the dispersion-relation model of Mahaux and collaborators [7], m_k has the same radial (r) dependence as the Hartree-Fock potential, whereas m_E is enhanced at the nuclear surface.

Only recently have $(e,e'p)$ data become available at large missing momentum p_m (corresponding to a large initial momentum of the struck proton) where such theoretical ideas can be tested. The $^{208}\mathrm{Pb}(e,e'p)$ cross sections measured by Bobeldijk *et al.* [9], for example, extend up to $p_m = 500$ MeV/c. Comparison of these data with various theoretical predictions [10–16] indicated that, whereas LRC were essential for understanding results obtained for low-lying final states in ^{207}Tl, SRC had little or no effect. On the other hand, for continuum final states [17] in ^{207}Tl the inclusion of both LRC and SRC seemed necessary to bring the calculations closer to the data, although a discrepancy persists that increases with excitation energy.

In this Letter we present a novel approach for comparing radial wave functions extracted from inelastic electron-scattering data and from electron-induced proton knockout data. Consider a pure $M\lambda$ transition, such as the $M3$ transition from the 3^+ ground state to the 0^+ excited state of ^{10}B at 1.74 MeV. In the single-particle model the ground state is described by a stretched $(1p_{3/2})^2$ configuration, and the excited state is reached by inverting the angular momentum of one nucleon. Thus, in the absence of $\geq 2\hbar\omega$ admixtures, the magnetic form factor for this transition is determined by a single-nucleon radial wave function, here denoted as $R_{e,e'}(r)$, such that

$$F_{M3}(q) \propto q \int_0^\infty [R_{e,e'}(r)]^2 j_2(qr) r^2 \, dr \,, \qquad (1)$$

where q is the momentum transfer. This equation can be inverted by standard techniques based on Fourier-Bessel transforms [18,19] to yield $R_{e,e'}(r)$. The results of such an analysis, including corrections for meson-exchange currents, were published recently [20,21].

Similarly, in the plane-wave impulse approximation (PWIA) the $(e,e'p)$ missing-momentum distribution for single-nucleon knockout from the same orbital is

 0031-9007/98/80(18)/3924(4)$15.00

described by the Fourier transform of an overlap function, here denoted as $R_{e,e'p}(r)$, such that

$$\rho(p_m) \propto \left| \int_0^\infty R_{e,e'p}(r) j_1(p_m r) r^2 \, dr \right|^2 . \qquad (2)$$

Thus, the radial overlap function can also be extracted from $(e, e'p)$ using Fourier-Bessel techniques. The dependence of $R_{e,e'p}(r)$ on the final state of the residual nucleus, with missing energy E_m, remains implicit.

At the level of the mean-field approximation, both radial functions would have the same form, such that $R_{e,e'}(r) \propto R_{e,e'p}(r) \propto \phi(r)$ where $\phi(r)$ is a normalized eigenfunction of the mean field. However, nonlocality corrections, correlations, and nuclear dynamics may have different effects on the radial functions appropriate to these two reactions. Hence, it is useful to introduce correction factors such that $R_\alpha(r) \propto \sqrt{\eta_\alpha(r)}\,\phi(r)$, where α distinguishes between reactions, namely, (e, e') or $(e, e'p)$. For example, according to Ma and Wambach [15,16] one should identify $\eta_{e,e'p}$ with an effective-mass correction to the quasiparticle wave function, $m^*(r, E_m)/m$. Similarly, one could argue that the form factor measured by electron scattering should be compared with a Hartree-Fock wave function, including the nonlocality correction represented by the k mass, that optimizes the single-particle model such that $\eta_{e,e'}$ corresponds to $m_k(r)/m$. Although we cannot justify such interpretations rigorously without further developments in many-body theory, it is reasonable to expect that the η factors for both reactions should approach unity at very large distances. Therefore, we define the nonlocality ratio

$$\kappa(r) = \frac{\eta_{e,e'p}(r)}{\eta_{e,e'}(r)} \propto \left(\frac{R_{e,e'p}(r)}{R_{e,e'}(r)} \right)^2 \qquad (3)$$

as the ratio between these η factors and require $\kappa \to 1$ for $r \to \infty$. Thus, if $\eta_{e,e'} \propto m_k(r)/m$ and $\eta_{e,e'p} \propto m^*(r, E_m)/m$, we would expect to find that the ratio of radial functions extracted from (e, e') and $(e, e'p)$ experiments resembles the E mass, such that $\kappa(r, E_m) \propto m_E(r, E_m)/m$.

The $^{10}\mathrm{B}(e, e'p)$ data employed to investigate these ideas were taken from an experiment performed at the medium-energy electron accelerator at NIKHEF. The energy, duty factor, and average current of the beam were 407.3 ± 0.2 MeV, 1%, and 1.5 μA, respectively. The target consisted of boron powder, enriched in ^{10}B, hot pressed with 2% polystyrene binder into a 1.3×3.8 cm^2 wafer of thickness 101.6 mg/cm^2. Scattered electrons and knocked-out protons were detected using two high-resolution magnetic spectrometers [22]. The measurements were performed in parallel kinematics, where the ejected proton is detected parallel to the momentum transfer $\vec{q}$. The outgoing proton energy in the center of momentum frame was kept constant at $T_{\mathrm{cm}} = 120$ MeV. Further details can be found elsewhere [23].

Separate runs were performed to calibrate the beam energy, spectrometer acceptances, and coincidence efficiency. The data were analyzed using methods described elsewhere [24], yielding a total systematic uncertainty of 5%–6%. The reduced cross section, defined as the sixfold differential cross section divided by the off-shell electron-proton cross section $\sigma_{\mathrm{ep}}^{\mathrm{cc1}}$ as given by De Forest [25] and by the appropriate kinematic factor, is shown in Fig. 1.

The spectrum exhibits two sharp peaks, corresponding to the $\frac{3}{2}^-$ ground state and the $\frac{5}{2}^-$ state at 2.429 MeV in ^{9}Be, followed by broad, overlapping resonances. A detailed analysis [23] showed that the spectrum is dominated by $\ell = 1$ knockout up to $E_x \simeq 19$ MeV, and by $\ell = 0$ knockout above that value.

Figure 2 shows momentum distributions obtained by integrating over the six main $\ell = 1$ structures in the spectrum. These are compared to two distorted-wave impulse approximation (DWIA) calculations [26–28] using different phenomenological and microscopic potentials [29]. For each of the $\ell = 1$ transitions it was found that the rms radius extracted for the overlap wave function was insensitive (<3%) to the description of final-state interaction (FSI) or other subtle effects. This lends confidence to the degree of model independence achieved in the determination of overlap wave functions from the $^{10}\mathrm{B}(e, e'p)$ data.

The next step in the analysis was to transform the data for the six $\ell = 1$ structures to r space. Distortions were first removed by multiplying the $(e, e'p)$ data with the ratio of PWIA to DWIA calculations, where the microscopic potential was used to compute the proton distortions. The resulting "plane wave" momentum distribution was then transformed using the Fourier-Bessel (FB) transformation code FOUBES [18,19]. Since the p_m range of our $^{10}\mathrm{B}(e, e'p)$ data is rather small (0–1.35 fm^{-1}) only a few FB coefficients are determined by the data. This can partly be remedied by choosing a large value for the cutoff radius, $R_{\mathrm{c}} = 11$ fm. Furthermore, the shapes of the fitted

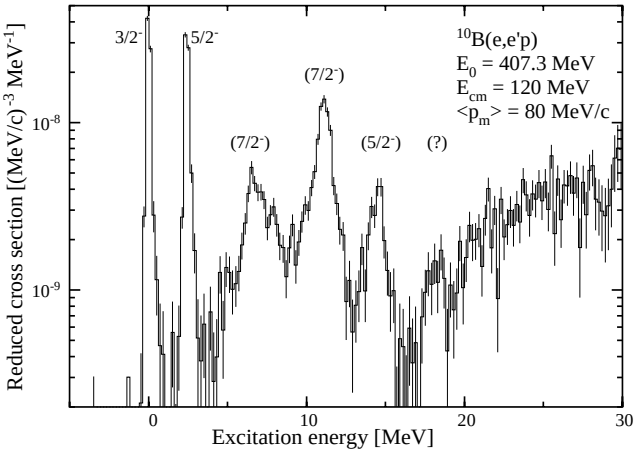

FIG. 1. $^{10}\mathrm{B}(e, e'p)$ excitation energy spectrum obtained at a missing momentum $\langle p_m \rangle = 80$ MeV/c. The main structures are labeled by their (tentative) spin-parity assignments.

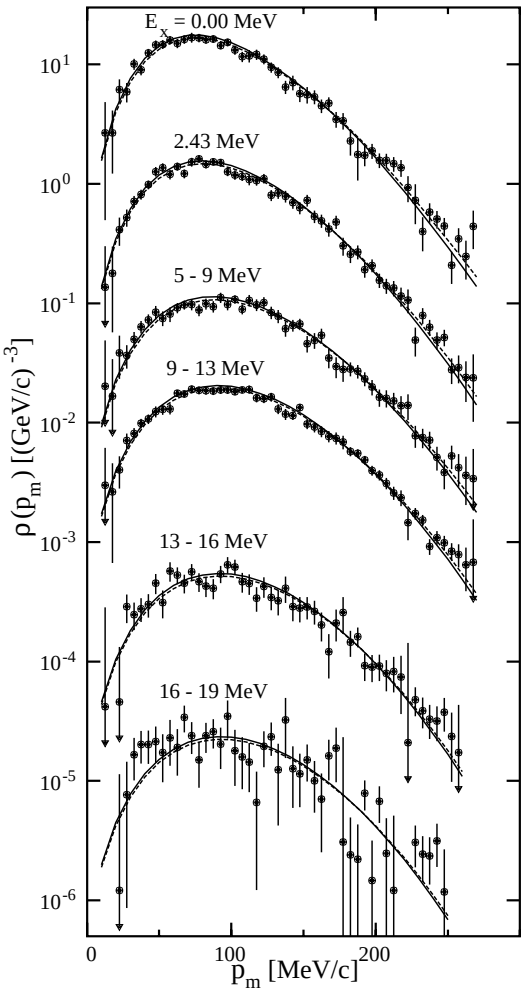

FIG. 2. ^{10}B$(e, e'p)$ momentum distributions for various E_x intervals, offset by successive powers of 10. The curves represent optical-model calculations performed with microscopic (solid lines) and phenomenological potentials (dashed lines).

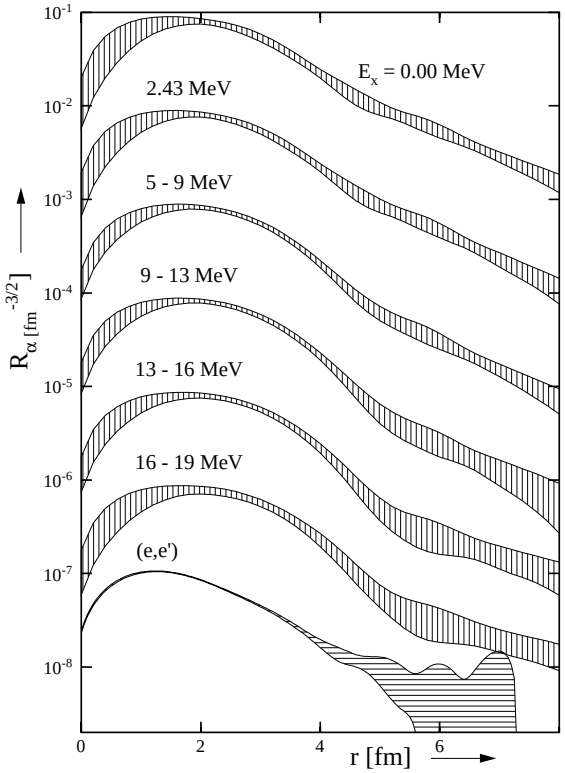

FIG. 3. The $1p\frac{3}{2}$ wave functions extracted from the ^{10}B$(e, e'p)$ data and (e, e') data (bottom curve) by means of the Fourier-Bessel technique for various E_x intervals. The abscissa represents the relative core-particle separation, and the normalization is such that $4\pi \int_0^\infty [R(r)]^2 r^2\, dr = 1$. The $(e, e'p)$ curves are offset by successive powers of 10.

wave functions have been biased with a Woods-Saxon dependence beyond $r = 6$ fm in order to damp oscillations that would occur in an unconstrained FB analysis.

The results are shown in Fig. 3, together with the $1p\frac{3}{2}$ wave function extracted from the ^{10}B(e, e') data [20,21]. Different radial sensitivities are observed for the ^{10}B(e, e') and $(e, e'p)$ data. By virtue of the existence of form factor data up to high momentum transfer, $q \simeq 4$ fm^{-1}, the (e, e') wave function is well determined in the nuclear interior. The $(e, e'p)$ wave functions, on the other hand, are better determined at the nuclear surface.

Finally, the nonlocality ratios $\kappa(r, E_m)$ were obtained by evaluating the experimental ratios $R_{e,e'p}(r)/R_{e,e'}(r)$. The $\kappa(r, E_m)$ data were fitted using a parametrization of the effective E mass suggested by Ma and Wambach [15,16], such that

$$\kappa(r, E_m) = 1 + \beta_v(E_m) g(r) + \beta_s(E_m) g'(r), \qquad (4)$$

where $g(r)$ is a Fermi function that approximately follows the radial density of ^{10}B. In this model, the free parameters $\beta_v(E_m)$ and $\beta_s(E_m)$ represent volume and surface effects, respectively. The normalization of $R_{e,e'p}(r)/R_{e,e'}(r)$ was also treated as a free parameter and used to enforce the constraint $\kappa(r, E_m) \to 1$ for large r. In order to obtain good fits to the data the radius parameter R, contained in $g(r)$, must be allowed to increase with E_m (from 2.6 to 3.4 fm). In Fig. 4 the experimental ratios for the six $\ell = 1$ regions are compared to fits based on Eq. (4). Note that the uncertainties related to the treatment of the FSI (see Fig. 2) and exchange currents [27,28] are small compared to the error bars displayed in Fig. 4. For small E_m we find that the volume effect dominates and that the nonlocality ratios exhibit a surprisingly strong central depression. As the missing energy increases, a strong enhancement of the $\kappa(r, E_m)$ develops at the surface while the interior depression decreases. This observation is independent of the normalization of $R_{e,e'p}$. Although this surface enhancement is qualitatively similar to the effective E mass proposed by Ma and Wambach for ^{208}Pb and ^{40}Ca [15,16], the effect we find for ^{10}B is considerably stronger. These results suggest that coupling to surface modes is stronger for light, highly deformed nuclei than for medium to heavy spherical nuclei.

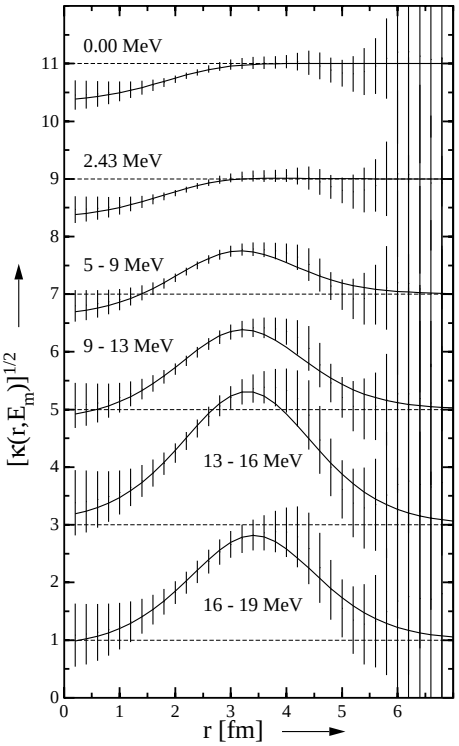

FIG. 4. The nonlocality ratio $\kappa(r, E_m)$ extracted from $^{10}\mathrm{B}(e, e'p)$ data. The various E_x intervals are vertically displaced from each other by 2 units. Also shown are fits based on a parametrization of the nucleon effective mass from Refs. [15,16].

In summary, it has been shown that ratios of $1p_{3/2}$ radial wave functions derived from precise $^{10}\mathrm{B}(e, e'p)$ and $^{10}\mathrm{B}(e, e')$ data evolve from an interior depression for small E_m to a surface-peaked enhancement for larger E_m. These observations can possibly be interpreted in terms of models of the quasiparticle effective mass, but both effects are stronger for $^{10}\mathrm{B}$ than expected from calculations for heavy nuclei.

This work is part of the research program of the FOM-institute for subatomic physics, NIKHEF, which is financially supported by the Netherlands' Organisation for Scientific Research (NWO). Additional support was received from NSF Grants No. PHY-9513924 (J. J. K.) and No. INT-9024674 (R. S. H.), the U.S. Department of Energy (R. S. H., R. A. M., and G. A. P.), and FWO-Flanders (D. V. N.).

[1] G. Jacob and Th. A. J. Maris, Nucl. Phys. **31**, 139 (1962); **31**, 152 (1962).
[2] S. Frullani and J. Mougey, Adv. Nucl. Phys. **14**, 1 (1984).
[3] L. Lapikás, in *Proceedings of the Fourth Workshop on Perspectives in Nuclear Physics at Intermediate Energies, ICTP, Trieste, 1989* (World Scientific, Singapore, 1989), p. 419.
[4] P. K. A. de Witt Huberts, J. Phys. G **16**, 507 (1990).
[5] G. van der Steenhoven, Nucl. Phys. **A527**, 17c (1991).
[6] L. Lapikás, Nucl. Phys. **A553**, 297c (1993).
[7] C. Mahaux and R. Sartor, Adv. Nucl. Phys. **20**, 1 (1991).
[8] J. J. Kelly, Adv. Nucl. Phys. **23**, 75 (1996).
[9] I. Bobeldijk *et al.*, Phys. Rev. Lett. **73**, 2684 (1994).
[10] V. R. Pandharipande, C. N. Papanicolas, and J. Wambach, Phys. Rev. Lett. **53**, 1133 (1984).
[11] V. R. Pandharipande and S. C. Pieper, Nucl. Phys. **A507**, 167c (1990).
[12] C. Mahaux and H. Ngo, Nucl. Phys. **A431**, 486 (1984).
[13] C. Mahaux, P. F. Bortignon, R. A. Broglia, and C. H. Dasso, Phys. Rep. **120**, 1 (1985).
[14] C. Mahaux and R. Sartor, Nucl. Phys. **A546**, 65c (1992).
[15] Z. Y. Ma and J. Wambach, Nucl. Phys. **A402**, 275 (1983).
[16] Z. Y. Ma and J. Wambach, Phys. Lett. B **256**, 1 (1991).
[17] I. Bobeldijk *et al.*, Phys. Lett. B **353**, 32 (1995).
[18] J. Heisenberg, Adv. Nucl. Phys. **12**, 61 (1981).
[19] J. Heisenberg and H. P. Blok, Annu. Rev. Nucl. Part. Sci. **33**, 569 (1983).
[20] R. S. Hicks, J. Button-Shafer, B. Debebe, J. Dubach, A. Hotta, R. L. Huffman, R. A. Lindgren, G. A. Peterson, R. P. Singhal, and C. W. de Jager, Phys. Rev. Lett. **60**, 905 (1988).
[21] A. Cichocki, J. Dubach, R. S. Hicks, G. A. Peterson, C. W. de Jager, H. de Vries, N. Kalantar-Nayestanaki, and T. Sato, Phys. Rev. C **51**, 2406 (1995).
[22] C. de Vries, C. W. de Jager, L. Lapikás, G. Luijckx, R. Maas, H. de Vries, and P. K. A. de Witt Huberts, Nucl. Instrum. Methods Phys. Res., Sect. A **223**, 1 (1984).
[23] L. J. de Bever, Ph.D. thesis, Utrecht University, 1993 (unpublished).
[24] J. W. A. den Herder, H. P. Blok, E. Jans, P. H. M. Keizer, L. Lapikás, E. N. M. Quint, G. van der Steenhoven, and P. K. A. de Witt Huberts, Nucl. Phys. **A490**, 507 (1988).
[25] T. de Forest, Jr., Nucl. Phys. **A392**, 232 (1983).
[26] S. Boffi, C. Giusti, and F. D. Pacati, Nucl. Phys. **A336**, 437 (1980).
[27] C. Giusti and F. D. Pacati, Nucl. Phys. **A473**, 717 (1987).
[28] C. Giusti and F. D. Pacati, Nucl. Phys. **A485**, 461 (1988).
[29] L. J. de Bever, H. P. Blok, J. Blouw, M. Fujiwara, K. Hosono, J. J. Kelly, S. Kuwamoto, L. Lapikás, G. van der Steenhoven, K. Takahisa, J. Takamatsu, and M. Yosoi, Nucl. Phys. **A579**, 13 (1994).